Denitrification of groundwater with pyrite and *Thiobacillus denitrificans*

Clara Torrentó [1,], Jordi Cama [1], Jordi Urmeneta [2], Neus Otero [3] and Albert Soler [3].*

(1) Hydrogeochemistry Group, Institute of Environmental Assessment and Water Research IDAEA, CSIC, C/Jordi Girona, 18-26, 08034 Barcelona, Spain. clara.torrento@idaea.csic.es, jordi.cama@idaea.csic.es

(2) Department of Microbiology and Biodiversity Research Institute (IRBio), University of Barcelona, Av. Diagonal 645, 08028 Barcelona, Spain. jurmeneta@ub.edu

(3) Mineralogia Aplicada i Medi Ambient Group, Department of Crystallography, Mineralogy and Ore Deposits, University of Barcelona, Martí i Franquès s/n, 08028 Barcelona, Spain. notero@ub.edu, albertsolergil@ub.edu

(*) Corresponding author: Clara Torrentó e-mail: clara.torrento@idaea.csic.es Fax: +34 93 411 00 12.

1

Abstract

Anaerobic batch and flow-through experiments were performed to confirm the role of pyrite as electron donor in bacterial denitrification and to look into the feasibility of pyrite-driven denitrification of nitrate-contaminated groundwater. Nitrate reduction was satisfactorily accomplished in experiments with pyrite as the sole electron donor, in presence of the autotrophic denitrifying bacterium *Thiobacillus denitrificans* and at nitrate concentrations comparable to those observed in contaminated groundwater. The experimental results corroborated field studies in which the reaction occurred in aquifers. Nitrate reduction rates and nitrate removal efficiencies were dependent on pyrite grain size, initial nitrate concentration, nitrate-loading rate and pH. The N and O isotopic enrichment factors (εN and εO) obtained experimentally for pyrite-driven nitrate reduction by *Thiobacillus denitrificans* ranged from -13.5‰ to -15.0‰ and from -19.0‰ to -22.9‰, respectively. These values indicated the magnitude of the isotope fractionation that occurs in nitrate-contaminated aquifers dominated by autotrophic denitrification.

Keywords: denitrification, pyrite, dissolution, *Thiobacillus denitrificans*, isotope fractionation.

1. INTRODUCTION

Groundwater contamination by nitrate usually originates from anthropogenic sources, mainly as a result of wastewater discharges and the intensive application of fertilizers and animal manure to agricultural land. It is not unusual for groundwater nitrate concentration to exceed the nominal limit of 50 mg L^{-1} set by the 98/83/EC European Union Council Directive.

Water remediation is necessary to prevent public-health and environmental impacts. The most significant natural attenuation process is denitrification, i.e. the reduction of nitrate to dinitrogen gas by anaerobic facultative bacteria (and a few archaea) that utilize nitrate as the electron acceptor (Knowles, 1982; Zumft, 1997). Bacteria that are capable of denitrification are ubiquitous with the result that denitrification occurs throughout terrestrial, freshwater, and marine systems where the following conditions arise simultaneously: (i) nitrate and electron donor availability, (ii) low oxygen concentrations (dissolved oxygen concentrations less than around 1-2 mg L^{-1}, Cey et al., 1999; Korom, 1992), and (iii) favorable environment (temperature, pH, other nutrients and trace elements). Denitrifying bacteria are generally heterotrophic and utilize organic matter as the electron donor. Nevertheless, a limited number of bacteria are capable of carrying out chemolithotrophic denitrification and of using inorganic compounds such as reduced sulfur compounds, hydrogen, ferrous iron or uranium (IV) as electron donors, and inorganic carbon (CO_2 or HCO_3) as the carbon source for cell material synthesis (Beller, 2005; Straub et al., 1996; Zumft, 1997). The obligate chemolithoautotrophic bacterium *Thiobacillus denitrificans* is well known for its ability to couple the oxidation of various sulfur and reduced iron compounds to denitrification (Beller et al., 2006).

A number of field studies have demonstrated the occurrence of natural denitrification coupled to oxidation of pyrite based on geochemical and/or isotopic data (Aravena and Robertson, 1998; Beller et al., 2004; Cravotta, 1998; Le Bideau and Dudoignon, 1996; Otero et al., 2009; Pauwels et al., 1998, 2000, 2010; Postma et al., 1991; Schwientek et al., 2008; Zhang et al., 2009). Denitrification by pyrite oxidation is expressed as:

$$14NO_3^- + 5FeS_2 + 4H^+ \Rightarrow 7N_2 + 10SO_4^{2-} + 5Fe^{2+} + 2H_2O \quad (1)$$

If the Fe^{2+} produced is oxidized:

$$NO_3^- + 5Fe^{2+} + 6H^+ \Rightarrow \frac{1}{2}N_2 + 5Fe^{3+} + 3H_2O \quad (2)$$

an overall reaction where denitrification mediated by pyrite oxidation occurs is expressed as:

$$15NO_3^- + 5FeS_2 + 10H_2O \Rightarrow \frac{15}{2}N_2 + 10SO_4^{2-} + 5Fe(OH)_3 + 5H^+ \quad (3)$$

Our interest is to characterize this pyrite-driven denitrification reaction and assess its feasibility. Although much work has been devoted to enhancing autotrophic denitrification by adding several inorganic electron donors, such as zero-valent iron, ferrous ions, elemental sulfur, and iron bearing materials (Benz et al., 1998; Choe et al., 2004; Hansen et al., 2001; Postma, 1990; Sierra-Alvarez et al., 2007; Soares, 2002; Straub et al., 1996; Weber et al., 2001), fewer studies have been carried out on nitrate reduction by pyrite and other sulfide minerals (Devlin et al., 2000; Haaijer et al., 2007; Jorgensen et al., 2009; Schippers and Jorgensen, 2002). In these studies, the role of pyrite as electron donor has been questioned and only in Jorgensen et al. (2009), has been denitrification coupled to pyrite oxidation satisfactorily accomplished. These authors performed pyrite-amended batch experiments with sediment from a sandy aquifer and demonstrated that addition of pyrite increased nitrate reduction rates. However, little is still known about the kinetics, the limiting factors and the

involvement of *T. denitrificans*-like bacteria in this reaction. Therefore, the first goal of this paper is to determine, clarify and quantify the role of pyrite as an electron donor in the bacterial mediated denitrification process in order to assess its feasibility for nitrate remediation in contaminated groundwater.

In addition, N and O isotope fractionation has been qualitatively used to study natural bacterially mediated nitrate reduction in contaminated aquifers (Otero et al., 2009). However, to quantify field denitrification, the enrichment factor (ε) must be determined with reasonable accuracy. N and O enrichment factors have been determined in groundwater field studies (Böttcher et al., 1990; Fukada et al., 2003; Mengis et al., 1999) and in laboratory pure culture experiments with denitrifying cultures (Barford et al., 1999; Delwiche and Steyn, 1970; Wellman et al., 1968). The latter studies are extremely useful because they provide a basis for the interpretation of field data, highlighting the magnitude of fractionation that could occur in different groups of microorganisms under specific biogeochemical conditions. These estimations have been performed with pure cultures of heterotrophic denitrifying bacteria. To our knowledge, isotope fractionation during autotrophic denitrification in laboratory cultures has not been reported to date. Therefore, the second goal of this study is to characterize nitrogen and oxygen isotope fractionation for pyrite-driven denitrification by *T. denitrificans* in order to evaluate the magnitude of the isotopic fractionation expected in nitrate-contaminated aquifers.

To accomplish both goals, two types of experiments with powdered pyrite were performed: (1) batch experiments inoculated with pure culture of *T. denitrificans* to study the overall reaction and determine isotope fractionation and (2) long-term flow-through experiments to evaluate the performance of the denitrification process over time and under flow conditions.

2. MATERIALS AND METHODS

2.1. Pyrite characterization and preparation

Natural pyrite crystals were obtained from sedimentary deposits in Navajún (Logroño, Spain) and from metasedimentary deposits in the Cerdanya region (Catalan Pyrenees, Spain). Powder X-ray diffraction of the samples was determined using a Bruker D5005 difractometer with Cu Kα radiation over a 2θ range from 0 to 60 degrees with a scan speed of 0.025°/18 s. The X-ray patterns confirmed the samples to be pyrite and showed no evidence of the presence of any other mineral phase. Based on electron microprobe analysis (EMPA), the Navajún pyrite atomic composition was 66.5 at.% of S and 33.3 at.% of Fe with impurities of Ni (0.07±0.05 at.%). The atomic composition of the Cerdanya pyrite was 66.5 at % of S and 33.3 at.% of Fe with impurities of Ni, Co and Cu (0.06±0.04, 0.04±0.06 and 0.04±0.03 at.%, respectively).

Pyrite samples were crushed and sieved to obtain two particle sizes, one ranging from 25 to 50 μm and the other from 50 to 100 μm. The samples used in two blank (TD-blank-21 and TD-blank-22, Table 1) and in two pyrite-amended (TD-13 and TD-14, Table 2) batch experiments were washed with 6 M HCl solution for 5 min and then rinsed with Milli-Q pure water three times before the start of the experiments to remove microparticles and possible iron and sulfur impurities on the pyrite surface. Specific surface areas were determined by the BET gas adsorption method with a Micromeritics ASAP 2000 surface area analyzer using 5-point N_2 adsorption isotherms (Brunauer et al., 1938). Initial surface areas for 25-50 μm particles were 0.59±0.06 $m^2\ g^{-1}$ for the Navajún pyrite and 0.88±0.09 $m^2\ g^{-1}$ for the Cerdanya pyrite (from here on all values are mean ± standard deviation unless otherwise noted). Surface areas for 50-100 μm particles were 0.43±0.04 $m^2\ g^{-1}$ and 0.62±0.06 $m^2\ g^{-1}$, respectively. After the

experiments, BET specific surface area of reacted samples was also measured. Pyrite powders for use in batch and inoculated flow-through experiments were sterilized by autoclave at 121°C for 15 min.

X-ray Photoelectron spectra (XPS) of initial and reacted samples were recorded with a Physical Electronics (PHI) 5500 spectrometer using a monochromatic X-ray source with an Al Kα line of 1486.6 eV energy and operated at 350 W. The energy scale was calibrated using the $3d_{5/2}$ line for Ag with a width of 0.8 eV and a binding energy of 368.3 eV. All binding energies were corrected by adjusting the C1s peak (corresponding to contamination from hydrocarbons) to a binding energy of 284.6 eV. Atomic concentrations of iron and sulfur were determined from the XPS areas subsequent to the Shirley background subtraction divided by atomic sensitivity factors (Wagner, 1983).

2.2. Culture preparation

Thiobacillus denitrificans (strain DSMZ No. 12475 from German Collection of Microorganisms and Cell Cultures, Germany) was cultured with thiosulfate in an anaerobic (pH 6.8) nutrient medium specially designed for *T. denitrificans*, following Beller (2005). The medium consisted of a mixed solution of $Na_2S_2O_3 \cdot 5H_2O$ (20 mM), NH_4Cl (18.7 mM), KNO_3 (20 mM), KH_2PO_4 (14.7 mM), $NaHCO_3$ (30 mM), $MgSO_4 \cdot 7H_2O$ (3.25 mM), $FeSO_4 \cdot 7H2O$ (0.08 mM), $CaCl_2 \cdot 2H_2O$ (0.05 mM) and sterile vitamin, trace element and selenate-tungstate solutions (stock solutions 1, 4, 6, 7 and 8 of Widdel and Bak, 1992). Cultures were maintained under anaerobic conditions at 30°C and unshaken. Thereafter, the culture was harvested by centrifugation, washed, and resuspended in sterile saline solution (Ringer 1/4 solution) immediately before the start of the experiments.

2.3. Experimental set-up

All the experiments were performed under anaerobic conditions in a sterilized and anaerobic glove box with a nominal gas composition of 90% N_2 and 10% CO_2 at 28±2 °C. Experimental oxygen partial pressure in the glove box was maintained between 0.1 and 0.3% O_2(g), being continuously monitored by an oxygen partial pressure detector with an accuracy of ±0.1% O_2(g). Input solutions were introduced into the glove box at least 12 h before the start of the experiments to allow equilibration with the anaerobic atmosphere and were sparged with N_2 for 15 min before the start of the experiments. The solutions to be autoclaved were degassed before the sterilization. All the experiments were set up with nitrate as the electron acceptor and pyrite as the sole electron donor. Pyrite was added in stoichiometric excess with respect to added nitrate.

Three types of batch experiments were performed: control experiments (Table 1), *T. denitrificans*-inoculated experiments amended with pyrite (Table 2), and experiments designed to calculate isotope fractionation (Table 3).

Two groups of independent control experiments were performed (Table 1): (1) pyrite-free experiments (both inoculated and non-inoculated) and (2) sterilized blank experiments with pyrite.

Pyrite-amended batch experiments were performed to confirm the occurrence of pyrite-driven nitrate reduction and to evaluate the nitrate removal rate by *T. denitrificans* (Table 2). Two groups of experiments were conducted with two different sizes of Navajún pyrite particles (25-50 and 50-100 μm). Each group included three different initial cell densities (approx. 10^5, 10^7 or 10^8 cells mL^{-1}). For each cell density, three different initial nitrate concentrations (approx. 1, 2.5 or 4 mM) were used. Each experiment performed with approximately 10^8 cells mL^{-1} was repeated 3-4 times in order to assess the reproducibility of the results (Table 2). 50 mL polypropylene bottles were filled with 25 mL of pH 6.8-7.0 modified medium with the desired concentration of nitrate, and 5 g of sterilized pyrite powder

141 with the desired grain size were added. The modified medium used in the batch experiments was the
142 *T. denitrificans* nutrient medium without thiosulfate and iron, replacing sulfate salts by chloride salts
143 and adding the desired nitrate concentration: NH_4Cl (18.7 mM), KH_2PO_4 (14.7 mM), $NaHCO_3$ (30
144 mM), $MgCl_2 \cdot 6H_2O$ (3.25 mM) and $CaCl_2 \cdot 2H_2O$ (0.05 mM) and the desired NO_3^- concentration as KNO_3.
145 Under these conditions pyrite will be the only electron donor available for the cells. Preliminary
146 experiments showed that initial pyrite-solution interaction caused a decrease in pH to below 6. This
147 was likely due to dissolution of surface grinding-resulted microparticles and possible surficial S-
148 impurities. This pH drop considerably diminished bacterial activity. Denitrification efficiency is very
149 sensitive to pH and an optimum pH range for most denitrifying bacteria is 7-8 (Knowles, 1982).
150 Therefore, after 24-42 h, the supernatant was eliminated and replaced by the fresh input solution.
151 After 48 h, aqueous samples corresponding to time 0 were collected and flasks were inoculated with 1
152 mL of cell solution with the desired cell density. To ensure that the possible presence of microparticles
153 and/or oxidation products on the pyrite surface has no significant effect on the rate and efficiency of
154 the reaction, two pyrite-amended experiments were performed with HCl-washed pyrite (TD-13 and
155 TD-14, Table 2).

156 In the experiments designed to characterize nitrogen and oxygen isotope fractionation associated
157 with the process (Table 3), the procedure was the same but using 250 mL glass Witeg bottles with 100
158 mL of solution and 20 g of pyrite; 4 mL of culture were inoculated into each flask.

159 Batch experiments were run for 14 d (25-50 μm pyrite) or for 60 d (50-100 μm pyrite and pyrite-free
160 experiments) and aqueous samples were periodically taken using sterile syringes. The number of
161 samples was limited to maintain the solid-solution ratio at < 30% of the initial value.

Flow-through experiments were performed to investigate pyrite-dependent denitrification under similar conditions to the natural environment and to evaluate the long-term performance of the process. Three types of flow-through experiments were performed: inoculated, blank and non-inoculated (Table 4). By means of a peristaltic pump, input solutions were circulated through 50 mL polyethylene reactors in which 50-100 μm powdered Cerdanya pyrite (approximately 1 g in the blank and non-inoculated experiments and 10 g in the inoculated experiment) was placed.

The *T. denitrificans*-inoculated experiment was carried out to evaluate the response and the denitrification capability of the pure culture over long term (several months). After 15 d of inoculation (6.6×10^7 cells mL^{-1}), solution was circulated through the reactor with a flow rate of 0.003 mL min^{-1}, yielding a hydraulic retention time (HRT) of 11.6 d. Reactors, tubing, pyrite powder and solutions were sterilized before use in the inoculated experiment and also in the blank experiment.

The non-inoculated experiments, with non-sterilized pyrite powder, were performed to stimulate activity of indigenous bacteria. The flow rate ranged between 0.009 and 0.014 mL min^{-1}, yielding HRT of 2.3-3.9 d. These non-inoculated experiments were replicated to ensure the reproducibility of the results (Table 4).

Input solution in the inoculated experiment was the modified *T. denitrificans* medium solution with 2.5 mM KNO_3 (nitrate loading rate of 0.21 mmol NO_3^- L^{-1} d^{-1}). Input solutions in the blank and non-inoculated experiments consisted of $NaNO_3$ solutions with nitrate concentration between 0.4 and 2.5 mM, yielding nitrate loading rates from 0.11 to 0.50 mmol NO_3^- L^{-1} d^{-1}. In the two solutions, no other electron donor was added to ensure that pyrite was the only electron donor available for cells. In order to ensure an optimal pH, pH of influent solutions was between 6.5 and 8. Nevertheless, one of

183 the non-inoculated experiments (NON-1, Table 4) was carried out at pH 4.5 to confirm the fatal effect
184 of pH on nitrate reduction.

185 Experimental runs lasted between 200 and 375 d and output solutions were collected periodically.

186 **2.4. Analytical methods**

187 Aliquots of aqueous samples were filtered through 0.22 μm syringe filters to measure pH,
188 concentrations of cations, anions, ammonium, and, in some samples, $\delta^{15}N$ and $\delta^{18}O$ of dissolved
189 nitrate. Samples were preserved in nitric acid to measure concentrations of total Fe, total S, Mg, Ca,
190 Na, Cl, P, and K by inductive coupled plasma-atomic emission spectrometry (ICP-AES, Thermo Jarrel-
191 Ash with CID detector and a Perkin Elmer Optima 3200 RL). The accuracy on the measurement of Mg,
192 Ca, Na, Cl, P and K was estimated to be around 3%, whereas the accuracy on the measurement of Fe
193 and S was estimated to be 25%, with detection limits of 0.36 and 3.12 μmol L^{-1}, respectively. Anion
194 concentrations (nitrate, nitrite, chloride, and sulfate) were determined by High Performance Liquid
195 Chromatography (HPLC), using an IC-Pack Anion column and borate/gluconate eluent with 12% of
196 HPLC grade acetonitrile. The error associated with the measurements was estimated to be 5% for
197 nitrate, chloride and sulfate and 10% for nitrite. Samples for ammonium analysis were preserved
198 acidified to pH<2 with H_2SO_4. Ammonium concentrations were measured using an Orion ammonium
199 ion selective electrode with an analytical uncertainty of 10% and a detection limit of 0.01 mM. pH was
200 measured with a calibrated Crison pH Meter at room temperature (22±2 °C). The pH error was 0.02
201 pH units.

202 Samples for N and O isotopes of nitrate were stored in KOH (pH 11) solution and frozen prior to
203 analysis. The $\delta^{15}N$ and $\delta^{18}O$ of dissolved nitrate were obtained following the denitrifier method

204 (Casciotti et al., 2002; Sigman et al., 2001). Notation is expressed in terms of δ per mil relative to the
205 international standards: V-SMOW (Vienna Standard Mean Oceanic Water) for $\delta^{18}O$ and AIR
206 (Atmospheric N_2) for $\delta^{15}N$. The isotope ratios were calculated using international and internal
207 laboratory standards. The results had an accuracy of 0.2 ‰ for $\delta^{15}N$ and 0.5 ‰ for $\delta^{18}O$ of nitrate.

208 **3. RESULTS AND DISCUSSION**

209 **3.1. Nitrate reduction**

210 In the control batch experiments, nitrate concentrations remained unchanged up to 60 d (Table 1).
211 Consumption of nitrate over time was only observed in the pyrite-amended, *T. denitrificans*-inoculated
212 batch experiments (Fig. 1). The time needed to consume nitrate was dependent on pyrite grain size
213 and initial nitrate concentration. In most of the experiments with 25-50 μm pyrite, nitrate content was
214 mostly consumed within 14 d (Fig. 1A). In cultures amended with 50-100 μm pyrite, the time needed
215 to consume most nitrate was longer and decreased by lowering the initial nitrate concentration. With
216 an initial concentration of approx. 4 mM NO_3^-, 35 to 80% of the nitrate content was consumed after 60
217 d; with approx. 2.5 mM NO_3^-, nitrate was completely consumed within 60 d; and with approx. 1 mM
218 of NO_3^-, complete consumption of nitrate occurred within 14 d (Fig. 1B).
219 An initial stage of 7 d during which nitrate concentration barely decreased was observed with the
220 lowest initial cell density (~10^5 cells mL^{-1}) (data not shown). This occurred because a longer adaptation
221 time was necessary for bacteria to grow into a population large enough to bring about a detectable
222 change in nitrate concentration. Nevertheless, the final percentages of reduced nitrate tended to
223 resemble those of experiments with higher initial cell density (Table 2).

As regards the flow-through experiments, nitrate reduction occurred in all the non-inoculated and inoculated experiments, but not in the blank experiment. In the *T. denitrificans*-inoculated experiment, partial nitrate removal occurred for 70 d (Fig. 2A). Subsequently, complete nitrate removal was achieved and lasted until the end of the experiment (200 d), indicating a high long-term efficiency of *T. denitrificans* in nitrate removal using pyrite as the electron donor under the study conditions. Figure 2B shows the consumption of nitrate in one representative non-inoculated flow-through experiment. In these experiments, a maximum nitrate reduction was achieved after 50-200 d (Table 4). Thereafter, nitrate content remained fairly constant until nitrate reduction slowed down to stop (e.g. NON-3a, Fig. 2B). Nonetheless, in some experiments after an apparent cessation of nitrate reduction, reduction restarted and high nitrate removal efficiency (expressed as the percentage of maximum nitrate removal) (60-94%) was finally attained (e.g. NON-2, Fig. 3A). In three experiments, a lag of approximately 80-100 d was observed before nitrate reduction started (e.g. NON-4a, Fig. 3B). In other experiments, nitrate reduction apparently did not cease during the duration of the tests (e.g. NON-4c, Fig. 3C). These behaviors could be attributed to shifts over the course of the runs in the composition of the dominant microbial community or in the enzyme regulation of the denitrifying organisms, probably as a result of changes in the experimental conditions that control the activity and growth of bacteria (such as oxygen concentration or nutrient availability). At pH 4.5 (NON-1), nitrate reduction was less effective than that observed in experiments carried out at pH 6.5-8, confirming the marked decrease in microbial activity due to acid pH (Table 4). Nitrate reduction efficiency was dependent on the nitrate loading rate. As is shown in the Table 4, when the nitrate loading rate ranged between 0.11 and 0.25 mmol NO_3^- L^{-1} d^{-1}, nitrate reduction was effective (overall nitrate removal of 40-80%), lasting

up to 150-350 d. By contrast, with high nitrate loading rates (0.33-0.50 mmol NO_3^- L^{-1} d^{-1}), nitrate reduction efficiency was lower (overall nitrate removal lower than 30%), lasting only 20-70 d (e.g. NON-6b, Fig. 3D). It should be noted that, although efficiency in nitrate removal was different, the maximum amount of nitrate removed was similar in the two cases (between 0.12 and 0.48 mM for lower nitrate loading rates and 0.31-0.38 mM for higher ones). Therefore, a maximum nitrate removal of 0.48 mM was attained, regardless of the input concentration of nitrate.

Nitrate reduction to diatomic nitrogen gas occurs in four steps, nitrite being one of the intermediate products. The basic nitrate reduction pathway is represented as $NO_3^- \rightarrow NO_2^- \rightarrow NO \rightarrow N_2O \rightarrow N_2$.

In most of the pyrite-amended batch experiments nitrite reduction took place rapidly and the final products were N-gaseous compounds (i.e. NO, N_2O or N_2). Furthermore, no changes in the ammonium concentration were detected over time, ruling out dissimilatory nitrate reduction to ammonium (Korom, 1992). Beller et al. (2006) showed that *T. denitrificans* has all the necessary genes encoding the four essential enzymes that catalyze denitrification. Our results confirm that these bacteria are able to reduce, at least, nitrate and nitrite. However, transient nitrite accumulation was evident in 6 batch experiments (TD-1a, TD-1b, TD-1c, TD-2a, TD-2b and TD-2c). Two examples are shown in Figure 1C. Peak nitrite concentrations were observed after 43 d, accounting for 15-35% of the initial nitrate concentration. Thereafter, nitrite concentration decreased. Nitrite was also present in some output solutions in the flow-through experiments. In the inoculated experiment, nitrite accumulated during the first 70 d, after which a complete nitrate removal was attained (Fig. 2A). In most of the non-inoculated flow-through experiments, nitrate reduction consisted of two stages. In the first stage, reduction products were nitrite and N-gaseous compounds, and in the second stage only

nitrite was produced before the denitrification ceased. An example is given in the Figure 4. As occurred in the batch experiments, dissimilatory nitrate reduction to ammonium could be excluded because ammonium concentrations in the output solutions were always below the detection limit.

In both the batch and flow-through experiments, nitrite accumulation resulted from the incomplete reduction of nitrate. Since pyrite was the sole electron donor and was placed in excess to avoid electron donor limitation, nitrite accumulation could be due to the competition between nitrate and nitrite reductases for the available electron donor. In this regard, high nitrate content has been found to inhibit nitrite reduction, inducing nitrite accumulation (Betlach and Tiedje, 1981; Blaszczyk, 1993; Thomsen et al., 1994; Van Rijn et al., 1996).

In summary, nitrate removal efficiency diminished as a result of an increase in nitrate concentration (i.e. nitrate loading rate) and in pyrite grain size, and as a result of a decrease in pH. A 100% efficiency in nitrate removal was achieved in the presence of *T. denitrificans*. Under non-sterilized, non-inoculated conditions, nitrate removal efficiency was lower, probably because of changes in the microbial population. Nitrite reduction yielded N-gaseous compounds although transient nitrite accumulation occurred in the open-system experiments.

3.2. Stoichiometry of the pyrite-driven denitrification process

In both batch and flow-through experiments, pyrite dissolution was confirmed by S release. The HPLC measurements for sulfate concentrations were concordant within ±5% with the sulfate concentrations calculated from ICP sulfur elemental data, assuming that concentrations of non-sulfate sulfur species (sulfides and sulfites) were negligible. In the batch experiments, an initial high S release was followed by a gradual S increase (Fig. 5A). This gradual S release started after time 0 and

289 occurred simultaneously to the reduction of nitrate in the inoculated experiments. The gradual
290 increase in S concentration was also observed in the blank experiments and it was in general lower
291 than in the inoculated experiments (Fig. 5A). This suggests that part of the S released in the inoculated
292 experiments could be attributed to pyrite oxidation by traces of dissolved oxygen as observed in the
293 blank experiments. Iron concentrations in all the batch experiments were below the detection limit,
294 given that reacting pH ranged between 6.5 and 7.5. In the flow-through experiments, output S
295 concentrations were higher at the start of the experiments, subsequently decreasing until a steady
296 state was attained (Fig. 5B). High concentrations at the start of the experiments were probably due to
297 dissolution of an outer layer of the reacting mineral or to dissolution of microparticles (Lasaga, 1998).
298 Iron concentrations were below the detection limit in all the flow-through experiments.
299 Therefore, the results of both batch and flow-through experiments show that nitrate reduction
300 occurred concurrently with the release of sulfate in the sterilized pyrite-amended experiments
301 inoculated with *T. denitrificans* and in the non-inoculated experiments with non-sterilized pyrite,
302 which showed inherent activity of indigenous bacteria. Under sterile conditions or under the
303 conditions of not adding pyrite, nitrate reduction did not occur. This indicates that nitrate reduction
304 was coupled with pyrite dissolution and was mediated by bacteria. Iron concentration was below
305 detection limit, suggesting that most of the Fe^{2+} resulting from pyrite oxidation was oxidized to Fe^{3+}
306 and precipitated. As stated in section 3.1, ammonium production could be excluded. Accordingly, the
307 overall reaction can be expressed as eq.(3).
308 If nitrate reduction was coupled to pyrite dissolution via eq. (3), the measured molar ratio of nitrate
309 consumed to sulfate produced should be close to the stoichiometric ratio of this reaction, which is 1.5.
310 However, in some experiments transient nitrite accumulation occurred, and therefore, the expected

311 nitrate/sulfate ratio was calculated based on the amount of nitrite accumulated according to the
312 following reaction:

313 $$15NO_3^- + 2FeS_2 + 7H_2O \Rightarrow 15NO_2^- + 4SO_4^{2-} + 2Fe(OH)_3 + 8H^+ \quad (4)$$

314 where nitrate/sulfate ratio is 3.75.

315 In most of the experiments, the final products of the overall reaction were gaseous N-compounds
316 (i.e. NO, N_2O or N_2). If the product was NO or N_2O, the nitrate/sulfate ratio should be 2.5 (eq. 5) and
317 1.9 (eq. 6), respectively:

318 $$15NO_3^- + 3FeS_2 + 3H_2O + 3H^+ \Rightarrow 15NO + 6SO_4^{2-} + 3Fe(OH)_3 \quad (5)$$

319 $$15NO_3^- + 4FeS_2 + \frac{13}{2}H_2O \Rightarrow \frac{15}{2}N_2O + 8SO_4^{2-} + 4Fe(OH)_3 + H^+ \quad (6)$$

320 In the inoculated pyrite-amended batch experiments, the nitrate/sulfate ratio was calculated using
321 sulfate released after time 0 given that nitrate reduction started after this time. The ratio ranged from
322 0.4 to 2.0, being lower than the possible stoichiometric ratios in most experiments (Table 2).
323 Nevertheless, the ratio was 1.5 within a 15% error in seven experiments. The low nitrate/sulfate ratio
324 indicates excess of sulfate, which, as stated above, could be explained by additional oxidation of pyrite
325 by traces of dissolved oxygen as observed in the blank experiments. In fact, the excess of sulfate
326 produced in the inoculated experiments (assuming that the reaction occurs via eq. 3) ranged from 0.2
327 to 5.0 mM in agreement with sulfate produced in the blank experiments (between 0.2 and 4.9 mM). It
328 is important to note that in the experiments in which pyrite was previously washed with HCl, the
329 molar nitrate/sulfate ratio was similar to that of the rest of the experiments, as occurred with the
330 efficiency and rate of nitrate removal (Table 2). This suggests that the presence of possible
331 microparticles and/or impurities on the pyrite surface had no significant effect on the overall process.

In the non-inoculated flow-through experiments, the measured nitrate/sulfate ratio at the time of maximum nitrate removal was significantly higher than the possible stoichiometric ratios (values higher than 10, Table 4). In fact, the percentage of nitrate reduction due to pyrite dissolution was calculated to be 1-30%. Moreover, this percentage could be lower since an amount of sulfate was released from dissolution of pyrite by traces of dissolved oxygen, as occurred in the blank flow-through experiments.

On the one hand, as pyrite powder and solutions were not previously autoclaved, a mixture of both autotrophic and heterotrophic denitrifying bacteria could have enhanced the denitrifying activity not linked to pyrite oxidation. The addition of pyrite as electron donor stimulated the activity of indigenous autotrophic denitrifying microorganisms and could also stimulate the activity of competing microbial populations, such as heterotrophic denitrifiers. Dead and lysed cells of the autotrophic bacteria could act as the carbon source for the heterotrophic bacteria since organic compounds were not provided (Koenig et al., 2005). However, it was difficult to estimate the amount of available C for heterotrophic denitrification over time and molecular analyses to identify the possible heterotrophic denitrifiers were not performed.

On the other hand, some deficit in sulfate, considering the expected sulfate production, could be partially attributed to passivation of the pyrite surface owing to precipitation of iron (hydr)oxide solid phases. XPS examination showed an enrichment of Fe onto the pyrite surface since surface Fe/S ratios increased from 0.50 to up to 0.77 (Table 5), which is consistent with the absence of iron in solution. Solution saturation indexes with respect to solid phases ($SI = \log(IAP/K_s)$, where SI is the saturation index, IAP is the ion activity product and K_s is the solid solubility product), and aqueous speciation of solutions were calculated using the code PHREEQC (Parkhurst, 1995) and the MINTEQ database.

PHREEQC calculations showed that the output solutions were supersaturated with respect to several iron oxy-hydroxides, such as goethite, ferrihydrite and $Fe(OH)_3$. Although aqueous iron was depleted, calculations were run by using a low iron concentration (1×10^{-3} mM). Nonetheless, part of this sulfate deficit could be attributed to the precipitation of S-rich secondary phases or elemental S as an intermediate phase.

In the inoculated flow-through experiment, the measured nitrate/sulfate ratio was also high (IN-1, Table 4). An iron coating may account for one part of the one part of the deficit in sulfate with respect to the expected sulfate production. XPS confirmed iron enrichment on the surfaces (Table 5) and, according to the PHREEQC calculations, output solutions were supersaturated with respect to iron oxy-hydroxides. However, it has been not possible to account for this discrepancy between the high amount of removed nitrate and the small concentration of released sulfate. One plausible reason could be heterotrophic contamination since aseptic conditions can be difficult to maintain in long-term, continuous-flow experiments inoculated with a pure culture (Claus and Kutzner, 1985).

3.3. Nitrate reduction rates

In pyrite-amended batch experiments, nitrate reduction rates were computed assuming zero-order kinetics and using linear regression to fit the remaining nitrate concentrations vs. time (Fig. 1). Computed nitrate reduction rates ranged between 0.09 to 3.50 mmol NO_3^- kg_{py}^{-1} d^{-1}, with $\sigma_{rate} \leq 20\%$ of rate in most cases (Table 2).

Nitrate reduction rates were higher in the experiments with 25-50 μm pyrite (2.12±0.83 mmol NO_3^- kg_{py}^{-1} d^{-1}) than in the 50-100 μm ones (0.39±0.31 mmol NO_3^- kg_{py}^{-1} d^{-1}). With initial nitrate concentration of approx. 1 mM, the nitrate reduction rate was higher than the rates with approx. 2.5 and 4 mM NO_3^-

375 (0.62±0.34, 0.19±0.01 and 0.28±0.23 mmol NO_3^- kg_{py}^{-1} d^{-1}, respectively). The variability in average rates
376 of the experiments with similar initial conditions (Table 2) could be attributed to different microbial
377 activity (especially in those experiments with low cell density) and/or certain degree of heterogeneity
378 in the range of grain size of the pyrite powders, which has been demonstrated to significantly modify
379 nitrate reduction rates and nitrate removal efficiency.

380 Rate dependence on pyrite grain size implies that the reduction rate depends on exposed pyrite
381 surface area. The larger the surface area, the higher the rate. A large surface area could enhance mass
382 transfer from solid surfaces to solution and/or bacterial attachment to the surface of pyrite grains.
383 Further experiments are necessary to ascertain whether the rate-limiting factor in the overall process is
384 mass transfer or bacterial adhesion.

385 In the flow-through experiments, the pyrite-mass normalized nitrate reduction rate, R_{NO3} (mol g^{-1} s^{-1})
386 was calculated from the maximum consumption of nitrate according to the expression:

387 $$R_{NO3} = \frac{q\,(C_{NO3} - C^{0}_{NO3})}{m} \qquad (7)$$

388 where q is the flow rate (L s^{-1}) of the solution through the reactor, C_{NO3} and C^{0}_{NO3} are the
389 concentrations (mol L^{-1}) of nitrate in the output and input solutions, respectively, and m is the pyrite
390 mass (g).

391 In the non-inoculated experiments, computed nitrate reduction rates ranged between 1.62 and 5.42
392 mmol NO_3^- kg_{py}^{-1} d^{-1} (Table 4). Lower nitrate reduction rate was computed in the experiment
393 performed at pH 4.5 (1.31 mmol NO_3^- kg_{py}^{-1} d^{-1}, Table 4). The nitrate loading rate faintly affected nitrate
394 reduction rates, although, as discussed above, nitrate reduction efficiency was higher in experiments
395 with low nitrate loading rates (0.11-0.25 mmol NO_3^- L^{-1} d^{-1}). The nitrate reduction rate obtained in the

inoculated experiment was 0.54 mmol NO_3^- kg_{py}^{-1} d^{-1}, which was lower than in the non-inoculated experiments although nitrate removal efficiency was higher in the former.

Hence, the results indicate that nitrate reduction rates increased by decreasing grain size and initial nitrate concentration. The nitrate reduction rates were lower in the inoculated flow-through experiment than in the non-inoculated ones, although efficiency in nitrate removal was higher in the former.

3.4. N and O isotope fractionation

During denitrification, as nitrate concentration decreases, residual nitrate becomes enriched in heavy isotopes ^{15}N and ^{18}O. When denitrification is treated as a single-step and unidirectional reaction in a closed system, the change in the isotopic composition of nitrate can be modeled using a Rayleigh-distillation type fractionation model (Mariotti et al., 1981):

$$\delta^{15}N_{residual} = \delta^{15}N_{initial} + \varepsilon_N \ln f \quad (10)$$

$$\delta^{18}O_{residual} = \delta^{18}O_{initial} + \varepsilon_O \ln f \quad (11)$$

where f is the unreacted portion of nitrate (residual nitrate concentration divided by the initial nitrate concentration), δ(residual) and δ(initial) are the nitrogen or oxygen isotopic compositions (‰) of the residual and initial nitrate, respectively, and ε (‰) is the isotopic enrichment factor. Accordingly, $\delta^{15}N$ and $\delta^{18}O$ of dissolved nitrate increase in proportion to the natural logarithm of the residual nitrate fraction.

Analysis of $\delta^{15}N$ and $\delta^{18}O$ of dissolved nitrate was carried out in two pyrite-amended batch experiments with 50-100 μm (TD-20) and 25-50 μm (TD-21) size fractions of pyrite (Table 3). The initial values of $\delta^{15}N_{NO3}$ and $\delta^{18}O_{NO3}$ were -2.3‰ and +25.1‰, respectively, and both values increased over

417 the experimental runs. In the 50-100 μm experiment, after 60 d, $\delta^{15}N_{NO3}$ and $\delta^{18}O_{NO3}$ increased to +8.4‰
418 and +34.9‰, respectively, with 52% reduction of initial nitrate. In the experiment with 25-50 μm
419 pyrite, after 16 d, $\delta^{15}N_{NO3}$ and $\delta^{18}O_{NO3}$ increased to +2.6‰ and +29.2‰, respectively, with 18%
420 reduction of initial nitrate. Figure 6A depicts $\delta^{15}N$ and $\delta^{18}O$ of the remaining nitrate vs. ln [NO_3^-] in
421 both experiments. In the 50-100 μm pyrite experiment, the values of εN and εO were -15.0‰ and
422 -13.5‰, respectively, based on the slope of the regression lines. In the experiment with 25-50 μm
423 pyrite, the values of εN and εO were -22.9‰ and -19.0‰, respectively. In both experiments, there is a
424 positive correlation ($r^2 > 0.99$) between $\delta^{15}N_{NO3}$ and $\delta^{18}O_{NO3}$, with slopes of 0.89 and 0.85, yielding
425 εN/εO ratios of 1.13 and 1.18, respectively (Fig. 6B).
426 To our knowledge, isotope fractionation during autotrophic denitrification in laboratory cultures
427 has not been reported to date. Therefore, the ε ranges obtained in this study using *T. denitrificans*
428 culture were compared with those reported in experiments with heterotrophic denitrifying strains
429 under different growth conditions (Table 6). However, it should be noted that the NO_3/SO_4 ratio of the
430 TD-20 experiment (2.8) was significantly higher than the stoichiometric ones, suggesting the possible
431 occurrence of heterotrophic contamination (Table 3). In this case, εN and εO could be associated with
432 a mixture of heterotrophic and autotrophic denitrification. These values cannot therefore be
433 unequivocally assigned to the denitrifying activity of *T. denitrificans*. The εN values obtained in this
434 study (-15.0‰ and -22.9‰) fall well within the range of values reported in the literature for nitrate
435 reduction to N_2 gas by heterotrophic denitrifying cultures (from -13.4‰ to -30.0‰, Delwiche and
436 Steyn, 1970; Wellman et al., 1968). Nonetheless, the values of εO (-13.5‰ and -19.0‰) were lower than
437 those reported by Toyoda et al. (2005) during the production of N_2O in acetylated experiments with 10
438 or 100 mM NO_3^- by two heterotrophic denitrifying pure cultures (-3‰ to +32‰). According to these

439 authors, two isotope effects with opposite $\delta^{18}O$ shifts may arise during nitrate reduction to nitrous
440 oxide: either (1) preferential reduction of the lighter molecules, which yields negative values of εO,
441 such as those obtained in the present study, or (2) preferential loss of ^{16}O during the enzymatic
442 reduction of nitrate, which results in an apparent 'inverse isotope effect' with positive values of O
443 fractionation (Casciotti et al., 2002; Toyoda et al., 2005). The coupled nitrate N and O isotope
444 fractionation during denitrification has been previously verified in field studies but not in laboratory
445 experiments with pure cultures of denitrifying bacteria. The εN/εO ratio obtained in this study
446 (1.15±0.04) is comparable to the ratios obtained from *in situ* studies of denitrification in groundwater,
447 which range from 0.9 to 2.3 (Otero et al., 2009 and references within). The εN/εO ratio is valuable to
448 trace biogeochemical processes in the N cycle. It allows to separate processes that overprint one
449 another when they are monitored using $\delta^{15}N$ alone, such as denitrification, nitrate assimilation by
450 plants, ammonification, nitrification, NH_3^+ volatilization, mixing processes, etc (Bottcher et al., 1990;
451 Mengis et al., 1999). Moreover, coupling nitrate N and O isotopes is used to estimate the intensity of
452 co-existing biogeochemical processes, to identify dominant sources of nitrate in natural waters
453 (Mengis et al., 2001) and to determine the fate of nitrate in areas with diffuse pollution (Otero et al.,
454 2009). Further laboratory studies with pure cultures of autotrophic and heterotrophic denitrifying
455 bacteria are required to evaluate the usefulness of the εN/εO ratio in the constraint or discrimination
456 between heterotrophic and autotrophic denitrification.

457 The N and O enrichment factors give an idea of the magnitude of the isotopic fractionation that
458 could be expected at field sites dominated by autotrophic denitrification based on pyrite oxidation,
459 such as the Osona aquifer (Otero et al., 2009). However, it should be noted that there is some
460 uncertainty about assigning the isotopic fractionation to denitrification performed exclusively by

461 autotrophic denitrifying bacteria. Further laboratory experiments with aquifer material are needed in
462 order to obtain enrichment factors that are characteristic for the specific aquifer.

463 **4. CONCLUSIONS**

464 Laboratory experiments were performed to clarify and characterize the role of pyrite in
465 denitrification in order to assess the feasibility of pyrite-driven denitrification of nitrate-contaminated
466 groundwater. Batch experiments were used to evaluate the ability of *T. denitrificans* to reduce nitrate
467 using pyrite and to determine associated N and O isotopic fractionation. Flow-through experiments
468 were carried out to explore pyrite-dependent denitrification under similar conditions to the natural
469 environment.

470 Inoculated experiments demonstrated that *T. denitrificans* is able to use pyrite as the electron donor
471 to reduce nitrate. Nitrate reduction rate was dependent on pyrite grain size, nitrate concentration and
472 pH. The results indicated that the extent and rate of denitrification increased as the size of pyrite
473 particles decreased. Moreover, 100% nitrate removal efficiency was achieved in long-term inoculated
474 flow-through experiments, which proves the long-term pyrite-driven denitrifying capacity of *T.*
475 *denitrificans*. Furthermore, inoculated batch experiments permitted to calculate N and O isotopic
476 enrichment factors for pyrite-driven nitrate reduction by *T. denitrificans*. To our knowledge, this is the
477 first study determining N and O isotope fractionation during denitrification by pure cultures of
478 autotrophic denitrifying bacteria. These values indicated the magnitude of the isotope fractionation
479 that occurs in nitrate-contaminated aquifers dominated by autotrophic denitrification.

480 Nitrate reduction also occurred under non-sterilized, non-inoculated conditions, but nitrate removal
481 efficiencies were lower and unpredictable denitrification stages were observed. Nevertheless, in three

experiments performed at low nitrate loading rate, almost 100% of nitrate removal was attained at the end (375 d). These results suggest that bacteria other than inoculated *T. denitrificans* were able to remove nitrate using pyrite at some stage. Furthermore, it should be noted that, although the bacterial community present in the non-inoculated experiments was not native to a nitrate contaminated aquifer, it was able to adapt to the new conditions and as a result reduce nitrate, probably by a combination of both autotrophic and heterotrophic denitrification.

Hence, the addition of pyrite to enhance activity of denitrifying bacteria could be considered for future water management strategies to remove nitrate at the concentrations commonly found in contaminated agricultural groundwater (up to 5 mM, e.g. Otero et al., 2009). However, a drawback of using the pyrite-driven denitrification process as a remediation strategy is at some extent the release of trace metals (e.g. As, Ni) and sulfate as a result of pyrite oxidation. Hence, care should be taken of the source and chemical characterization of the pyrite used as amendment. Furthermore, increasing the sulfate content in groundwater could contribute to eutrophication of surface waters (Smolders et al., 2006; Haaijer et al., 2007) and sulfate discharge into freshwater might require post-treatment processing. Future experiments using sediments from nitrate-contaminated aquifers should address denitrification enhancement by addition of pyrite to stimulate indigenous denitrifying bacteria.

Acknowledgments

This work was funded by projects CICYT-CGL2008-06373-C03-01 and TRACE PET 2008-0034 of the Spanish Government and the project 2009 SGR 103 from the Catalan Government. We thank the Serveis Científics Tècnics of the Universitat de Barcelona and the Woods Hole Oceanographic Institution for their services. We also thank Vanessa Ouro from the Institute of Environmental

503 Assessment and Water Research (CSIC) and Josep Elvira from the Institute of Earth Sciences "Jaume
504 Almera" (CSIC) for analytical assistance. We thank to George Von Knorring for improving the English
505 style of this paper. We are grateful to two anonymous reviewers and Associate Editor, Dr. Jeremy Fein
506 for their constructive comments and suggestions that significantly improved the original manuscript.

507 **REFERENCES**

508 Aravena, R., Robertson, W.D., 1998. Use of multiple isotope tracers to evaluate denitrification in
509 ground water: Study of nitrate from a large-flux septic system plume. Ground Water 36(6),
510 975-981.
511 Barford, C.C., Montoya, J.P., Altabet, M.A., Mitchell, R., 1999. Steady-state nitrogen isotope effects of
512 N_2 and N_2O production in *Paracoccus denitrificans*. Appl. Environ. Microbiol. 65(3), 989-994.
513 Beller, H.R., 2005. Anaerobic, nitrate-dependent oxidation of U(IV) oxide minerals by the
514 chemolithoautotrophic bacterium *Thiobacillus denitrificans*. Appl. Environ. Microbiol. 71(4),
515 2170-2174.
516 Beller, H.R., Chain, P.S.G., Letain, T.E., Chakicherla, A., Larimer, F.W., Richardson, P.M., Coleman,
517 M.A., Wood, A.P., Kelly, D.P., 2006. The genome sequence of the obligately
518 chemolithoautotrophic, facultatively anaerobic bacterium *Thiobacillus denitrificans*. J. Bacteriol.
519 188(4), 1473-1488.
520 Beller, H.R., Madrid, V., Hudson, G.B., McNab, W.W., Carlsen, T., 2004. Biogeochemistry and natural
521 attenuation of nitrate in groundwater at an explosives test facility. Appl. Geochem. 19(9), 1483-
522 1494.
523 Benz, M., Brune, A., Schink, B., 1998. Anaerobic and aerobic oxidation of ferrous iron at neutral pH by
524 chemoheterotrophic nitrate-reducing bacteria. Arch. Microbiol. 169(2), 159-165.
525 Betlach, M.R., Tiedje, J.M., 1981. Kinetic explanation for accumulation of nitrite, nitric oxide, and
526 nitrous oxide during bacterial denitrification. Appl. Environ. Microbiol. 42(6), 1074-1084.

527 Blaszczyk, M., 1993. Effect of medium composition on the denitrification of nitrate by *Paracoccus*
528 *denitrificans*. Appl. Environ. Microbiol. 59(11), 3951-3953.
529 Böttcher, J., Strebel, O., Voerkelius, S., Schmidt, H.L., 1990. Using isotope fractionation of nitrate
530 nitrogen and nitrate oxygen for evaluation of microbial denitrification in a sandy aquifer. J.
531 Hydrol. 114(3-4), 413-424.
532 Brunauer, S., Emmett, P.H., Teller, E., 1938. Adsorption of gases in multimolecular layers. J. Am.
533 Chem. Soc. 60(2), 309-319.
534 Bryan, B.A., Shearer, G., Skeeters, J.L., Kohl, D.H., 1983. Variable expression of the nitrogen isotope
535 effect associated with denitrification of nitrite. J. Biol. Chem. 258(14), 8613-8617.
536 Casciotti, K.L., Sigman, D.M., Hastings, M.G., Bohlke, J.K., Hilkert, A., 2002. Measurement of the
537 oxygen isotopic composition of nitrate in seawater and freshwater using the denitrifier
538 method. Anal. Chem. 74(19), 4905-4912.
539 Cey, E.E., Rudolph, D.L., Aravena, R., Parkin, G., 1999. Role of the riparian zone in controlling the
540 distribution and fate of agricultural nitrogen near a small stream in southern Ontario. J.
541 Contam. Hydrol. 37(1-2), 45-67.
542 Claus, G., Kutzner, H.J., 1985. Physiology and kinetics of autotrophic denitrification by *Thiobacillus*
543 *denitrificans*. Appl. Microbiol. Biotechnol. 22(4), 283-288.
544 Cravotta, C.A., 1998. Effect of sewage sludge on formation of acidic ground water at a reclaimed coal
545 mine. Ground Water 36(1), 9-19.
546 Choe, S.H., Ljestrand, H.M., Khim, J., 2004. Nitrate reduction by zero-valent iron under different pH
547 regimes. Appl. Geochem. 19(3), 335-342.
548 Delwiche, C.C., Steyn, P.L., 1970. Nitrogen isotope fractionation in soils and microbial reactions.
549 Environ. Sci. Technol. 4(11), 929-935.
550 Devlin, J.F., Eedy, R., Butler, B.J., 2000. The effects of electron donor and granular iron on nitrate
551 transformation rates in sediments from a municipal water supply aquifer. J. Contam. Hydrol.
552 46(1-2), 81-97.
553 Fukada, T., Hiscock, K.M., Dennis, P.F., Grischek, T., 2003. A dual isotope approach to identify
554 denitrification in groundwater at a river-bank infiltration site. Water Res. 37(13), 3070-3078.

555 Haaijer, S.C.M., Lamers, L.P.M., Smolders, A.J.P., Jetten, M.S.M., Op de Camp, H.J.M., 2007. Iron
556 sulfide and pyrite as potential electron donors for microbial nitrate reduction in freshwater
557 wetlands. Geomicrobiol. J. 24(5), 391-401.
558 Hansen, H.C.B., Guldberg, S., Erbs, M., Koch, C.B., 2001. Kinetics of nitrate reduction by green rusts -
559 effects of interlayer anion and Fe(II): Fe(III) ratio. Appl. Clay Sci. 18(1-2), 81-91.
560 Jorgensen, C.J., Jacobsen, O.S., Elberling, B., Aamand, J., 2009. Microbial oxidation of pyrite coupled to
561 nitrate reduction in anoxic groundwater sediment. Environ. Sci. Technol. 43(13), 4851-4857.
562 Knowles, R., 1982. Denitrification. Microbiol. Rev. 46(1), 43-70.
563 Koenig, A., Zhang, T., Liu, L., Fang, H., 2005. Microbial community and biochemistry process in
564 autosulfurotrophic denitrifying biofilm. Chemosphere 58(8), 1041-1047.
565 Korom, S.F., 1992. Natural denitrification in the saturated zone - A review. Water Resour. Res. 28(6),
566 1657-1668.
567 Lasaga, A.C., 1998. Kinetic Theory in the Earth Sciences. Princeton University Press, Princeton, New
568 Jersey, 728 pp.
569 Le Bideau, L., Dudoignon, P., 1996. Evidence of natural denitrification mechanism at Beuxes (Vienne,
570 France). C.R. Acad. Sci., Ser. IIa: Sci. Terre Planets 322, 555-562.
571 Mariotti, A., Germon, J.C., Hubert, P., Kaiser, P., Létolle, R., Tardieux, A., Tardieux, P., 1981.
572 Experimental determination of nitrogen kinetic isotope fractionation - Some principles -
573 Illustration for the denitrification and nitrification processes. Plant Soil 62(3), 413-430.
574 Mengis, M., Walther, U., Bernasconi, S.M., Wehrli, B., 2001. Limitations of using $\delta^{18}O$ for the source
575 identification of nitrate in agricultural soils. Environ. Sci. Technol. 35(9), 1840-1844.
576 Mengis, M., Schif, S.L., Harris, M., English, M.C., Aravena, R., Elgood, R.J., MacLean, A., 1999.
577 Multiple geochemical and isotopic approaches for assessing ground water NO_3 elimination in
578 a riparian zone. Ground Water 37(3), 448-457.
579 Otero, N., Torrentó, C., Soler, A., Menció, A., Mas-Pla, J., 2009. Monitoring groundwater nitrate
580 attenuation in a regional system coupling hydrogeology with multi-isotopic methods: The case
581 of Plana de Vic (Osona, Spain). Agric., Ecosyst. Environ. 133(1-2), 103-113.

582 Parkhurst, D.L., 1995. User's guide to PHREEQC--A computer program for speciation, reaction-path,
583 advective-transport, and inverse geochemical calculations. U.S. Geological Survey Water-
584 Resources Investigations Report 95-4227, 143 pp.
585 Pauwels, H., Ayraud-Vergnaud, V., Aquilina, L., Molénat, J., 2010. The fate of nitrogen and sulfur in
586 hard-rock aquifers as shown by sulfate-isotope tracing. Appl. Geochem. 25(1), 105-115.
587 Pauwels, H., Foucher, J.C., Kloppmann, W., 2000. Denitrification and mixing in a schist aquifer:
588 influence on water chemistry and isotopes. Chem. Geol. 168(3-4), 307-324.
589 Pauwels, H., Kloppmann, W., Foucher, J.C., Martelat, A., Fritsche, V., 1998. Field tracer test for
590 denitrification in a pyrite-bearing schist aquifer. Appl. Geochem. 13(6), 767-778.
591 Postma, D., 1990. Kinetics of nitrate reduction by detrital Fe(II)-silicates. Geochim. Cosmochim. Acta
592 54(3), 903-908.
593 Postma, D., Boesen, C., Kristiansen, H., Larsen, F., 1991. Nitrate reduction in an unconfined sandy
594 aquifer - Water chemistry, reduction processes and geochemical modeling. Water Resour. Res.
595 27(8), 2027-2045.
596 Schippers, A., Jorgensen, B.B., 2002. Biogeochemistry of pyrite and iron sulfide oxidation in marine
597 sediments. Geochim. Cosmochim. Acta 66(1), 85-92.
598 Schwientek, M., Einsiedl, F., Stichler, W., Stögbauer, A., Strauss, H., Maloszewski, P., 2008. Evidence
599 for denitrification regulated by pyrite oxidation in a heterogeneous porous groundwater
600 system. Chem. Geol. 255(1-2), 60-67.
601 Shearer, G., Kohl, D.H., 1988. Nitrogen isotopic fractionation and ^{18}O exchange in relation to the
602 mechanism of denitrification of nitrite by *Pseudomonas stutzeri*. J. Biol. Chem. 263(26), 13231-
603 13245.
604 Sierra-Alvarez, R., Beristain-Cardoso, R., Salazar, M., Gómez, J., Razo-Flores, E., Field, J.A., 2007.
605 Chemolithotrophic denitrification with elemental sulfur for groundwater treatment. Water
606 Res. 41(6), 1253-1262.
607 Sigman, D.M., Casciotti, K.L., Andreani, M., Barford, C., Galanter, M., Bohlke, J.K., 2001. A bacterial
608 method for the nitrogen isotopic analysis of nitrate in seawater and freshwater. Anal. Chem.
609 73(17), 4145-4153.

610 Smolders, A.J.P., Lamers, L.P.M., Lucassen, E.C.H.E.T., Van Der Velde, G., Roelofs, J.G.M., 2006.
611 Internal eutrophication: How it works and what to do about it - A review. Chem. Ecol. 22(2),
612 93-111.
613 Soares, M.I.M., 2002. Denitrification of groundwater with elemental sulfur. Water Res. 36(5), 1392-
614 1395.
615 Straub, K.L., Benz, M., Schink, B., Widdel, F., 1996. Anaerobic, nitrate-dependent microbial oxidation
616 of ferrous iron. Appl. Environ. Microbiol. 62(4), 1458-1460.
617 Sutka, R.L., Ostrom, N.E., Ostrom, P.H., Breznak, J.A., Gandhi, H., Pitt, A.J., Li, F., 2006.
618 Distinguishing nitrous oxide production from nitrification and denitrification on the basis of
619 isotopomer abundances. Appl. Environ. Microbiol. 72(1), 638-644.
620 Thomsen, J.K., Geest, T., Cox, R.P., 1994. Mass spectrometric studies of the effect of pH on the
621 accumulation of intermediates in denitrification by *Paracoccus denitrificans*. Appl. Environ.
622 Microbiol. 60(2), 536-541.
623 Toyoda, S., Mutobe, H., Yamagishi, H., Yoshida, N., Tanji, Y., 2005. Fractionation of N_2O isotopomers
624 during production by denitrifier. Soil Biol. Biochem. 37(8), 1535-1545.
625 Van Rijn, J., Tal, Y., Barak, Y., 1996. Influence of volatile fatty acids on nitrite accumulation by a
626 *Pseudomonas stutzeri* strain isolated from a denitrifying fluidized bed reactor. Appl. Environ.
627 Microbiol. 62(7), 2615-2620.
628 Wagner, C.D., 1983. Sensitivity factors for XPS analysis of surface atoms. J. Electron. Spectrosc. Relat.
629 Phenom. 32(2), 99-102.
630 Weber, K.A., Picardal, F.W., Roden, E.E., 2001. Microbially catalyzed nitrate-dependent oxidation of
631 biogenic solid-phase Fe(II) compounds. Environ. Sci. Technol. 35(8), 1644-1650.
632 Wellman, R.P., Cook, F.D., Krouse, H.R., 1968. Nitrogen-15: Microbiological alteration of abundance.
633 Science 161(3838), 269-270.
634 Widdel, F., Bak, F., 1992. Gram-negative mesophilic sulfate-reducing bacteria, in: A. Balows, H.G.T.,
635 M. Dworkin, W. Harper and K.-H. Schleifer (Ed.), The Prokaryotes. Springer Verlag, New
636 York, pp. 3352-3378.

637 Zhang, Y.-C., Slomp, C.P., Broers, H.P., Passier, H.F., Cappellen, P.V., 2009. Denitrification coupled to
638 pyrite oxidation and changes in groundwater quality in a shallow sandy aquifer. Geochim.
639 Cosmochim. Acta 73(22), 6716-6726.
640 Zumft, W.G., 1997. Cell biology and molecular basis of denitrification. Microbiol. Mol. Biol. Rev. 61(4),
641 533-616.
642

643 **FIGURE CAPTIONS**

644 **Figure 1**. Variation of nitrate concentration over time in representative pyrite-amended batch
645 experiments inoculated with *T. denitrificans*. (A) Consumption of nitrate over time in the experiments
646 performed with approx. 2.5 mM NO_3^- solution; (B) Consumption of nitrate over time in the
647 experiments amended with 50-100 μm pyrite and inoculated with approx. 10^8 cells mL^{-1}; (C) NO_3^- and
648 NO_2^- concentration vs. time of experiments TD-1c and TD-2c; Solid lines represent the fitting of
649 measured NO_3^- concentration versus time used to compute zero-order nitrate reduction rates.
650 Determination coefficients (R^2) were ≥ 0.9 except in 2 experiments.

651 **Figure 2**. Variation of NO_3^- and NO_2^- concentration vs. time in input (i) and output (o) solutions of two
652 representative flow-through experiments. See Table 4. (A) Experiment inoculated with *T. denitrificans*
653 culture (IN-1); (B) One non-inoculated experiment (NON-3a). The ellipse shows the nitrate
654 concentration values used to calculate nitrate reduction rate (see eq. 7).

655 **Figure 3**. Variation of nitrate and nitrite concentration over time in input (i) and output (o) solutions of
656 four representative non-inoculated flow-through experiments. See Table 4. (A) Experiment NON-2.
657 Nitrate reduction apparently ceased after 230 d, but 10 d later, it restarted and about 94% nitrate
658 removal efficiency was achieved at the end (370 d). (B) Experiment NON-4a. In contrast to other non-
659 inoculated experiments, a lag of approx. 80 d was observed before nitrate reduction started. (C)
660 Experiment NON-4c. Nitrate reduction started at 50 d and did not cease during the duration of the
661 run (350 d). (D) NON-6b, performed with high nitrate loading rate (0.34 mmol NO_3^- L^{-1} d^{-1}). In contrast
662 to the experiments with lower nitrate loading rate, nitrate removal was less effective and lasted only
663 30 d.

Figure 4. Variation of nitrate and nitrite concentration over time in input (i) and output (o) solutions of one of the non-inoculated flow through-experiments (NON-3b). (A) Evolution of nitrate and nitrite concentrations. (B) Evolution of the sum of nitrate and nitrite concentrations in the output solutions. Nitrate reduction commenced at the start of the experiment and lasted 120 d. In the first 70 d, nitrate was reduced to nitrite, which in turn, reduced to a N-gaseous compound. Thereafter, between 70 and 120 d, nitrate reduced to nitrite, and nitrite was not reduced. After 120 d, nitrate reduction ceased.

Figure 5. Variation of S concentration over time in batch and flow-through experiments. (A) S concentration vs. time in representative blank and inoculated pyrite-amended experiments. Solid lines represent the fitting of measured and S concentration versus time used to compute zero-order S production rates, r_s. (B) S concentration vs. time in one representative flow-through experiment.

Figure 6. Isotopic results of the two pyrite-amended batch experiments inoculated with *T. denitrificans* and focusing on calculate isotope fractionation: TD-21 (with 25-50 μm pyrite) and TD-20 (50-100 μm pyrite). (A) $\delta^{15}N$ (filled symbols) and $\delta^{18}O_{NO3}$ (open symbols) vs. $\ln[NO_3^-]$. Values of εN and εO were obtained from the slope of the regression lines; (B) $\delta^{18}O$ vs. $\delta^{15}N_{NO3}$. Determination coefficients (R^2) ranged from 0.889 to 0.993 in both figures.

Figure 1

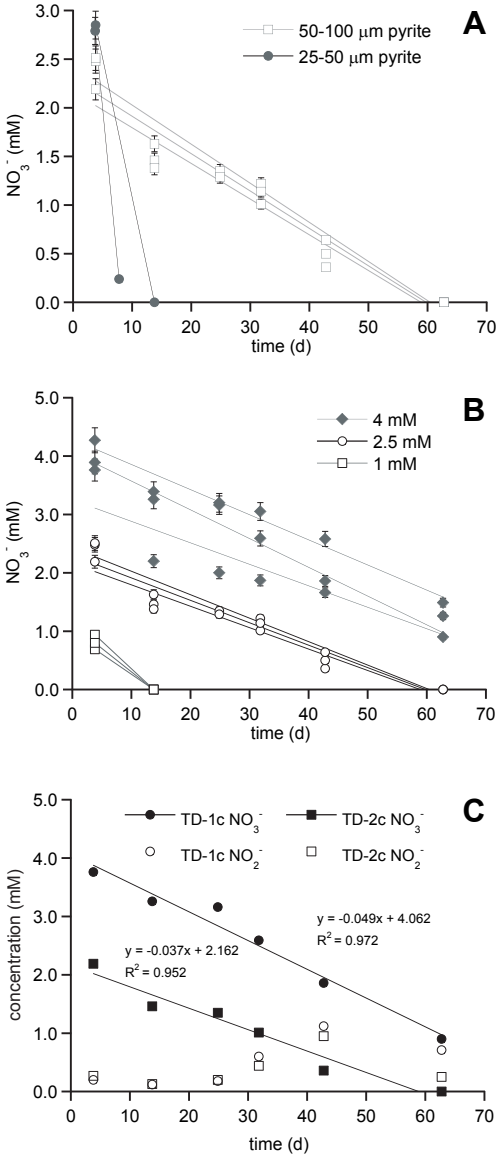
A
50-100 μm pyrite
25-50 μm pyrite
NO3- (mM)
time (d)
B
4 mM
2.5 mM
1 mM
NO3- (mM)
time (d)
C
TD-1c NO3-
TD-2c NO3-
TD-1c NO2-
TD-2c NO2-
y = -0.049x + 4.062
R2 = 0.972
y = -0.037x + 2.162
R2 = 0.952
concentration (mM)
time (d)

Figure 2

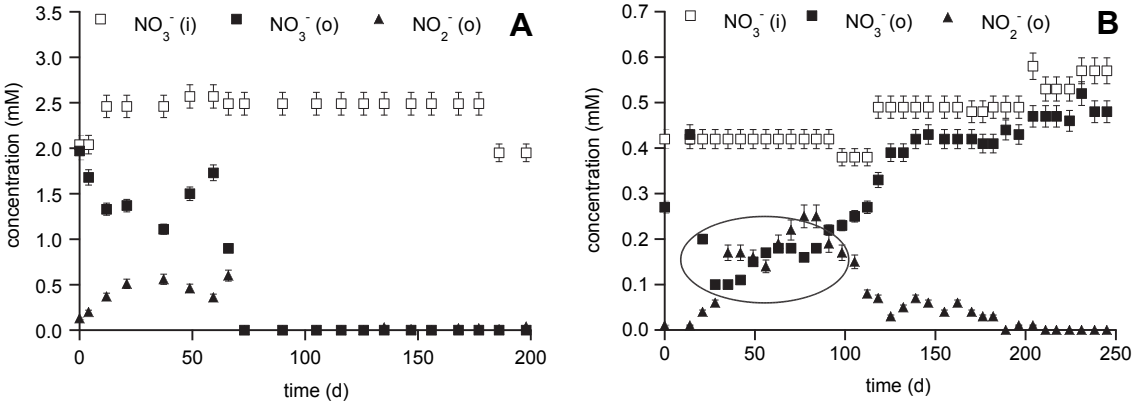
A
B
NO3- (i)
NO3- (o)
NO2- (o)
concentration (mM)
time (d)
0.0
0.5
1.0
1.5
2.0
2.5
3.0
3.5
0.1
0.2
0.3
0.4
0.6
0.7
0
50
100
150
200
250

Figure 3

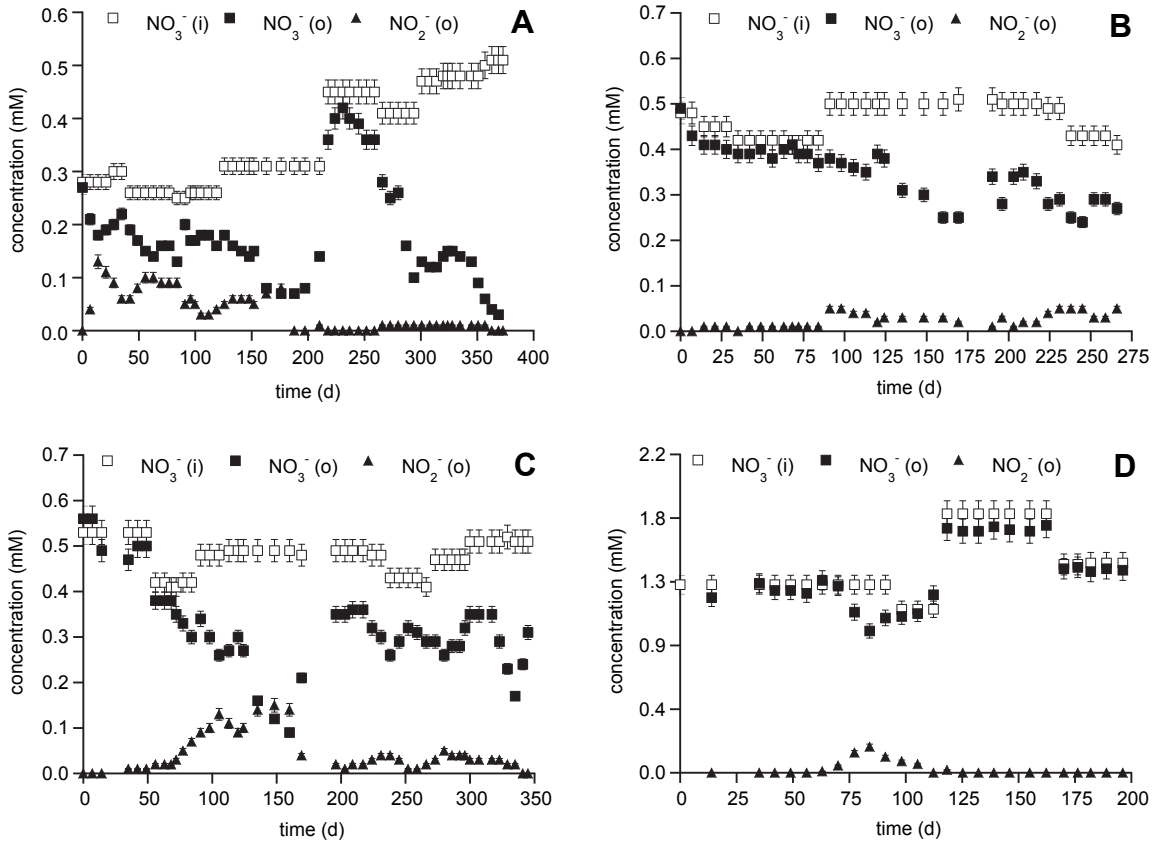

Figure 4

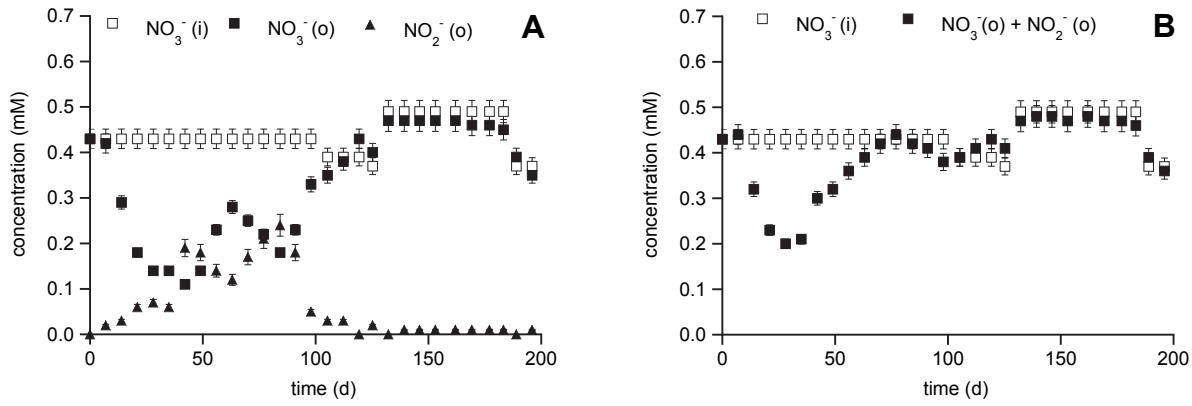
A
B
NO3- (i)
NO3- (o)
NO2- (o)
NO3-(o) + NO2- (o)
concentration (mM)
time (d)
0.0
0.1
0.2
0.3
0.4
0.5
0.6
0.7
0
50
100
150
200

Figure 5

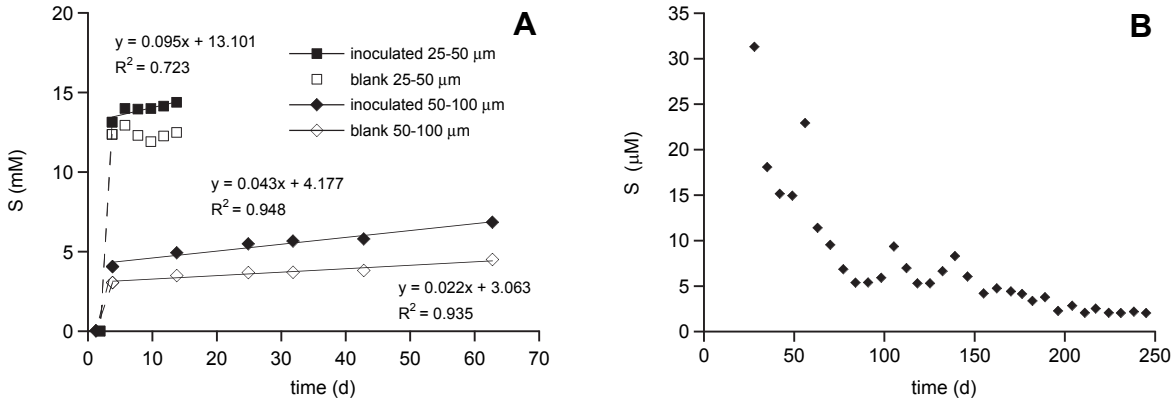
A
y = 0.095x + 13.101
R2 = 0.723
inoculated 25-50 µm
blank 25-50 µm
inoculated 50-100 µm
blank 50-100 µm
y = 0.043x + 4.177
R2 = 0.948
y = 0.022x + 3.063
R2 = 0.935
S (mM)
time (d)
B
S (µM)
time (d)

Figure 6

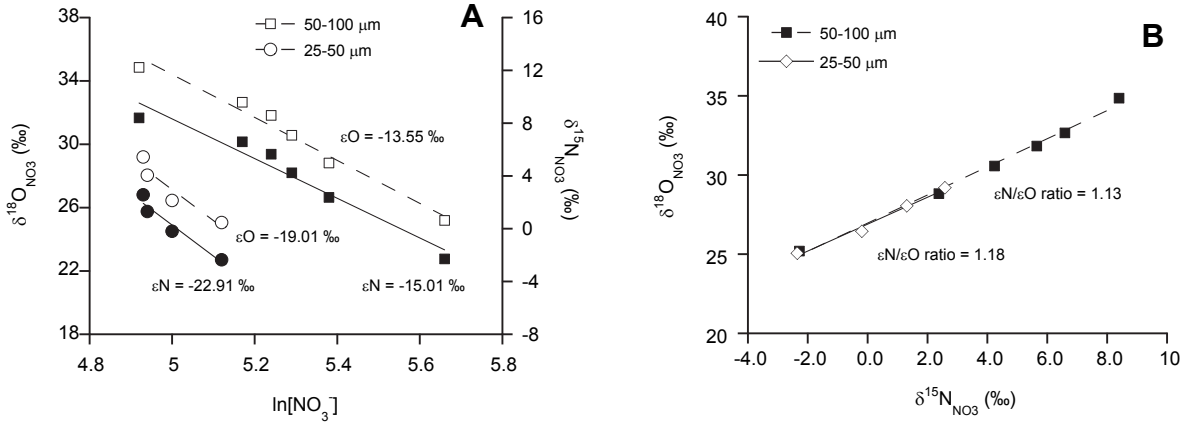
A
50-100 μm
25-50 μm
εO = -13.55 ‰
εO = -19.01 ‰
εN = -22.91 ‰
εN = -15.01 ‰
δ18ONO3 (‰)
δ15NNO3 (‰)
ln[NO3-]
B
50-100 μm
25-50 μm
εN/εO ratio = 1.13
εN/εO ratio = 1.18
δ18ONO3 (‰)
δ15NNO3 (‰)

Table 1. Experimental conditions and results of the control batch experiments

exp.	inoculum	grain size	initial nitrate	final nitrate (1)	final BET	sulfate produced (2)
	cells mL^{-1}	μm	mM	mM	$m^2 g^{-1}$	mM
Pyrite-free experiments						
TD-control-10	~10^7	-	4.46	4.50	-	-
TD-control-9	~10^7	-	4.37	4.31	-	-
TD-control-15	~10^7	-	4.31	4.29	-	-
TD-control-11	~10^5	-	4.58	4.57	-	-
TD-control-12	~10^5	-	4.57	4.31	-	-
TD-control-16	~10^7	-	3.76	3.34	-	-
TD-control-17	-	-	5.14	4.98	-	-
TD-control-13	-	-	4.75	4.84	-	-
TD-control-14	-	-	4.75	4.83	-	-
TD-control-18	-	-	4.40	4.19	-	-
TD-control-7	-	-	4.24	4.21	-	-
TD-control-8	-	-	3.78	4.09	-	-
Blank experiments with pyrite						
TD-blank-17	-	50-100	5.08	5.15	0.61	0.25
TD-blank-23	-	50-100	4.97	5.02	0.27	0.69
TD-blank-16	-	50-100	4.92	5.16	0.40	3.17
TD-blank-24	-	50-100	4.54	4.54	0.22	0.53
TD-blank-8	-	50-100	4.31	4.36	0.79	1.45
TD-blank-10	-	50-100	2.90	2.69	0.53	1.38
TD-blank-11	-	50-100	2.71	2.74	0.91	1.95
TD-blank-12	-	50-100	2.71	2.79	0.52	2.00
TD-blank-9	-	50-100	2.58	2.75	0.55	1.25
TD-blank-13	-	50-100	1.08	0.94	0.64	3.26
TD-blank-22 (3)	-	25-50	5.15	5.12	1.89	0.43
TD-blank-21 (3)	-	25-50	5.06	5.08	0.78	0.25
TD-blank-19	-	25-50	5.04	5.05	1.05	0.56
TD-blank-18	-	25-50	3.52	3.62	1.09	0.82
TD-blank-15	-	25-50	1.52	1.43	1.46	4.93
TD-blank-14	-	25-50	0.99	1.08	1.85	0.70

(1) After 60 d in pyrite-free experiments and in blank experiments with 50-100 μm pyrite and after 14 d in blank experiments with 25-50 μm pyrite

(2) From time 0 to 60 d (50-100 μm pyrite) or from 0 to 14 d (25-50 μm pyrite)

(3) Pyrite samples were previously washed with 6M HCl

Table 2. Experimental conditions and results of the pyrite-amended batch experiments inoculated with *T. denitrificans*

variable	exp.	initial nitrate	final nitrate (1)	final BET	overall NO_3^- removal (1)	NO_3^- reduction rate		sulfate produced (3)	NO_3 / SO_4 ratio (4)
		mM	mM	$m^2\ g^{-1}$	%	mmol NO_3^- $kg^{-1}\ d^{-1}$	σ rate (2)	mM	
50-100 μm									
~10^8 cells mL^{-1}									
~4 mM NO_3^-	TD-1a	3.89	1.26	0.65	68	0.18	0.06	6.75	0.4
	TD-1b	3.89	1.49	0.67	62	0.22	0.02	1.97	1.2
	TD-1c	3.76	0.90	0.81	76	0.25	0.02	1.73	1.7
	mean±SD	3.85±0.08	1.22±0.30	0.71±0.09	69±7	0.22±0.03		3.48±2.83	1.1±0.7
~2.5 mM NO_3^-	TD-2a	2.51	0.00	0.47	100	0.20	0.02	2.79	0.9
	TD-2b	2.48	0.00	0.79	100	0.19	0.03	2.94	0.8
	TD-2c	2.18	0.00	0.66	100	0.18	0.02	2.43	0.9
	mean±SD	2.39±0.18	0.00	0.64±0.17	100	0.19±0.01		2.72±0.26	0.9±0.0
~1 mM NO_3^-	TD-3a	0.94	0.00	0.64	100	0.47 (5)	-	0.81	1.2
	TD-3b	0.80	0.00	0.72	100	0.40 (5)	-	1.88	0.4
	TD-3c	0.90	0.00	0.56	100	0.45 (5)	-	2.18	0.4
	TD-3d	0.69	0.00	0.74	100	0.35 (5)	-	2.05	0.3
	mean±SD	0.83±0.11	0.00	0.67±0.09	100	0.42±0.06		1.73±0.62	0.6±0.4
~10^7 cells mL^{-1}									
~4 mM NO_3^-	TD-4	4.38	1.17 (6)	1.15	73 (6)	0.76	0.15	1.89	1.7
	TD-5	3.82	2.50	0.53	35	0.12	0.02	2.84	0.5
~1 mM NO_3^-	TD-6	1.06	0.00	1.12	100	1.23 (5)	-	1.19	0.9
	TD-7	0.66	0.00	1.04	100	0.81 (5)	-	0.41	1.6
~10^5 cells mL^{-1}									
~4 mM NO_3^-	TD-8	4.44	3.64 (6)	0.45	19 (6)	0.09	0.02	0.95	0.8
	TD-9	3.71	2.09	0.45	44	0.38	0.11	4.24	0.4
25-50 μm									
~10^8 cells mL^{-1}									
~4 mM NO_3^-	TD-10	4.76	0.00	1.27	100	2.28 (5)	-	3.98	1.2
~2.5 mM NO_3^-	TD-11	2.85	0.00	1.34	100	1.43 (5)	-	2.76	1.0
~10^7 cells mL^{-1}									
~4 mM NO_3^-	TD-12	4.29	2.15	0.56	50	1.06	0.08	1.24	1.7
	TD-13 (7)	3.94	0.88	1.02	78	1.40	0.13	1.52	2.0
	TD-14 (7)	3.72	0.00	0.90	100	2.50	0.22	3.68	1.0
	TD-15	3.32	0.00	0.34	100	3.50	0.69	3.06	1.2
~4 mM NO_3	TD-16	2.79	0.00	0.36	100	3.16 (5)	-	2.13	1.3
~10^5 cells mL^{-1}									
~4 mM NO_3^-	TD-17	3.79	0.55	0.33	86	1.71	0.28	2.56	1.3
	TD-18	3.52	0.00	1.59	100	2.09	0.55	2.67	1.3

(1) After 60 d in experiments with 50-100 μm pyrite and after 14 d in experiments with 25-50 μm pyrite

(2) Standard deviation of the linear regression of nitrate concentration over time (Fig. 1)

(3) From 0 to 60 d (50-100 μm pyrite) or from 0 to 14 d (25-50 μm pyrite)

(4) Ratio between measured nitrate reduced and sulfate produced

(5) Apparent nitrate reduction rates. Complete nitrate removal was detected at first sampling

(6) After 25 d in experiment TD-4 and after 42 d in experiment TD-8

(7) Pyrite samples were previously washed with 6M HCl

Table 3. Experimental conditions and results of the two pyrite-amended batch experiments inoculated with approximately 10^7 cells mL^{-1} *T. denitrificans* culture focusing on calculate isotope fractionation

exp.	grain size	initial nitrate	final nitrate (1)	final BET	overall NO_3^- removal (1)	NO_3^- reduction rate		sulfate produced (3)	NO_3 / SO_4 ratio (4)
	μm	mM	mM	$m^2\ g^{-1}$	%	mmol NO_3^- $kg^{-1}\ d^{-1}$	σ rate (2)	mM	
TD-20	50-100	4.61	2.20	0.31	52	0.19	0.03	0.87	2.8
TD-21	25-50	2.71	2.22	0.48	18	0.19	0.04	1.84	0.3

(1) After 60 d in experiment TD-20 and after 14 d in experiment TD-21

(2) Standard deviation of the linear regression of nitrate concentration over time (Fig. 1)

(3) From 0 to 60 d (TD-20) or from 0 to 14 d (TD-21)

(4) Ratio between measured nitrate reduced and sulfate produced

Table 4. Experimental conditions and results of blank, inoculated and non-inoculated flow-through experiments

exp.	nitrate input [1]	HRT	nitrate loading rate	output pH	final BET	pyrite mass	max. nitrate reduced	max. nitrate removal	nitrate reduction rate	S (s.s.)	Fe (s.s.)	NO_3 / SO_4 ratio [2] [3]	% NO_3^- reduced due to pyrite oxidation [3] [4]	comments
	mM	d	mmol NO_3^- L^{-1} d^{-1}		m^2 g^{-1}	g	mM	%	mmol NO_3^- kg^{-1} d^{-1}	µmol L^{-1}				
Sterilized blank experiment														
BLANK-1	0.43	3.1	0.14	7.2	0.50	0.79	-	-	-	1.58	b.d.l.	-	-	
Inoculated experiment														
IN-1	2.46	11.6	0.21	7.0	0.77	10.00	2.46	100	0.54	2.18	b.d.l.	24	6-10	Complete nitrate removal at 70 d. Lasted until the end (200 d)
Non-inoculated experiments														
NON-1	0.42	3.2	0.13	4.5	0.44	1.00	0.10	23	1.31	2.35	1.50	18	8-14	Maximum nitrate removal at 50 d. Nitrate reduction stopped at 75 d
NON-2	0.31	2.7	0.11	7.0	0.40	0.99	0.24	78	4.03	2.67	b.d.l.	40	5-7	Maximum nitrate removal at 175 d. Nitrate reduction stopped at 230 d. Nitrate removal restarted at 240 d and 94% of reduction at the end (370 d)
NON-3a	0.42	3.1	0.13	7.0	0.48	1.00	0.32	77	3.88	2.25	b.d.l.	18	12-17	Maximum nitrate removal at 35 d. Nitrate reduction stopped at 230 d
NON-3b	0.43	3.9	0.11	7.0	0.53	1.00	0.32	75	3.30	4.62	b.d.l.	23	10-14	Maximum nitrate removal at 40 d. Nitrate reduction stopped at 120 d
NON-3c	0.42	3.5	0.12	7.5	0.49	1.00	0.29	69	3.00	1.29	b.d.l.	17	14-18	Maximum nitrate removal at 40 d. Nitrate reduction stopped at 140 d. Nitrate removal restarted at 160 d and 60% of reduction at the end (250 d)
NON-3d	0.43	3.9	0.11	7.5	0.51	1.00	0.21	49	2.38	2.34	b.d.l.	10	18-28	Maximum nitrate removal at 20 d. Nitrate reduction stopped at 75 d. Nitrate removal restarted at 120 d and 60% of reduction at the end (240 d)
NON-3e	0.40	2.3	0.17	6.7	0.53	0.80	0.18	42	3.34	3.87	b.d.l.	59	4-5	Initial stage of 50 d with 1.1 mM NO_3^- input. Maximum nitrate removal at 85 d. Nitrate reduction stopped at 110 d
NON-3f	0.44	2.5	0.18	7.5	0.34	1.00	0.28	57	5.68	1.32	b.d.l.	>150	1-2	Initial stage of 65 d with pH3 HCl input. Maximum nitrate removal at 195 d. Nitrate reduction did not cease and 60% of reduction at the end (365 d)
NON-4a	0.46	3.4	0.14	7.3	0.50	0.99	0.26	51	2.57	2.00	b.d.l.	>150	1-2	Lag of 85 d before nitrate reduction started. Maximum nitrate removal at 130 d. Nitrate reduction did not cease
NON-4b	0.48	2.7	0.18	7.0	0.31	0.99	0.26	55	3.68	1.33	b.d.l.	>150	1	Initial stage of 200 d with 1.0 mM NO_3^- input. Maximum nitrate removal at 330 d. Nitrate reduction did not cease and 98% of reduction at the end (380 d)
NON-4c	0.49	2.9	0.17	7.4	0.29	1.00	0.40	81	4.85	1.56	b.d.l.	>150	1-2	Maximum nitrate removal at 160 d Nitrate reduction did not cease
NON-4d	0.50	3.2	0.16	7.7	0.32	1.00	0.12	28	1.62	2.15	b.d.l.	>150	1-2	Initial stage of 65 d with 1.0 mM NO_3^- input. Maximum nitrate removal at 165 d. Nitrate reduction did not cease and 83% of reduction at the end (240 d)
NON-4e	0.53	2.7	0.20	7.4	4.58	0.79	0.32	66	5.42	4.62	b.d.l.	>150	1-3	Maximum nitrate removal at 130 d. Nitrate reduction did not cease and 98% of reduction at the end (335 d)
NON-5a	0.86	3.5	0.25	7.2	0.64	1.01	0.48	49	3.81	1.84	b.d.l.	79	2-4	Lag of 90 d before nitrate reduction started. Maximum nitrate removal at 195 d. Nitrate reduction did not cease
NON-5b	0.88	3.5	0.25	7.3	0.41	1.01	0.43	41	3.78	3.45	b.d.l.	77	2-4	Lag of 100 d before nitrate reduction started. Maximum nitrate removal at 195 d. Nitrate reduction did not cease

NON-6a	1.29	3.9	0.33	7.5	0.62	1.00	0.38	29	2.57	2.20	b.d.l.	86	3-4	Maximum nitrate removal at 90 d. Nitrate reduction stopped at 160 d
NON-6b	1.30	3.9	0.34	7.2	0.60	1.00	0.32	24	3.89	3.11	b.d.l.	43	5-7	Maximum nitrate removal at 85 d. Nitrate reduction stopped at 105 d
NON-7	1.72	3.5	0.50	7.0	0.34	1.00	0.31	18	4.45	3.36	b.d.l.	57	3-5	Maximum nitrate removal at 90 d. Nitrate reduction stopped at 120 d

b.d.l. = below detection limit (3.12 μmol L^{-1} S; 0.36 μmol L^{-1} Fe)

HRT = hydraulic retention time

s.s. = steady state

(1) Nitrate average concentration of the input solution over the whole experiment

(2) Ratio between measured nitrate reduced and sulfate produced

(3) At time of maximum nitrate removal

(4) Based on the amount of nitrate reduced, sulfate and nitrite produced and the stoichiometry of the eqs. (3-6)

Table 5. Results obtained from X-ray Photoelectron Spectroscopy (XPS) determinations on the initial and reacted pyrite samples of some flow-through experiments. Surface stoichiometry is represented by molar ratios. Atomic concentrations of Fe and S in the pyrite surfaces were estimated by normalizing out the remaining elements (oxygen and adventitious carbon)

sample	Fe	S	Fe / S
	at. %		
Initial	33.5	66.5	0.50
NON-6b	39.1	60.9	0.64
NON-3b	43.6	56.4	0.77
IN-1	58.8	41.2	1.42

Table 6. Comparison between the enrichment factors for ^{15}N and ^{18}O estimated in laboratory experiments with pure heterotrophic denitrifying cultures reported in the literature with those estimated in the present study using *T. denitrificans*

species	system	εN (‰)	εO (‰)	εN / εO	reference	comments
Heterotrophic denitrifying bacteria						
Paracoccus denitrificans	$NO_3^- \rightarrow N_2O$	-28.6 ± 1.9	n.d.	n.d.	Barford et al. (1999)	steady-state reactor, acetate as electron donor, 30 mM NO_3^-
Paracoccus denitrificans	$N_2O \rightarrow N_2$	-12.9 ± 5.8	n.d.	n.d.		
Pseudomonas denitrificans	$NO_3^- \rightarrow N_2$	-13.4 to -20.8	n.d.	n.d.	Delwiche and Steyn (1970)	batch, glucose as electron donor
Pseudomonas stutzeri	$NO_3^- \rightarrow N_2$	-20 to -30	n.d.	n.d.	Wellman et al. (1968)	batch, 0.01 to 0.03 mM NO_3^-
Pseudomonas chlororaphis	$NO_3^- \rightarrow N_2O$	-12.7	n.d.	n.d.	Sutka et al. (2006)	batch, citrate as electron donor, 10 mM NO_3^-
Pseudomonas aerofaciens	$NO_3^- \rightarrow N_2O$	-36.7	n.d.	n.d.		
Pseudomonas fluorescens	$NO_3^- \rightarrow N_2O$	-39 to -31 (1)	+13 to +32 (1)	n.d.	Toyoda et al. (2005)	batch, citrate as electron donor, acetylated, 10 to 100 mM NO_3^-
	$NO_3^- \rightarrow N_2O$	-22 to -17 (1)	-3 to -1 (1)	n.d.		
Paracoccus denitrificans	$NO_3^- \rightarrow N_2O$	-22 to -10 (1)	+4 to +23 (1)	n.d.		
Pseudomonas stutzeri	$NO_2^- \rightarrow N_2$?	-5 to -20	n.d.	n.d.	Bryan et al. (1983)	batch, succinate as electron donor, 0.07 to 2.2 mM NO_2^-
Pseudomonas stutzeri	$NO_2^- \rightarrow N_2O$	-9.9 to -19.6	n.d.	n.d.	Shearer and Kohl (1988)	batch, succinate as electron donor, 0.1 to 2.3 mM NO_2^-
Autotrophic denitrifying bacteria						
Thiobacillus denitrificans	$NO_3^- \rightarrow N_2$?	-22.9 (2)	-19.0 (2)	1.18	this study (TD-21)	batch, 25-50 μm pyrite as electron donor, 2.7 mM NO_3^-
Thiobacillus denitrificans	$NO_3^- \rightarrow N_2$?	-15.0 (2)	-13.5 (2)	1.13	this study (TD-20)	batch, 50-100 μm pyrite as electron donor, 4.6 mM NO_3^-

(1) εN (or εO) calculated as difference between $\delta^{15}N_{N2O}$ (or $\delta^{18}O_{N2O}$) and $\delta^{15}N_{NO3}$ (or $\delta^{18}O_{NO3}$)

(2) see text for details